Molecular Modeling of Phenothiazine Derivatives: Self-Assembling Properties

Attila Bende,*,† Ion Grosu,‡ and Ioan Turcu†

Molecular and Biomolecular Physics Department, National Institute for Research and Development of Isotopic and Molecular Technologies, Donath Street, Number 65-103, Ro-400293 Cluj-Napoca, Romania and Chair of Organic Chemistry, Faculty of Chemistry and Chemical Engineering, "Babeş-Bolyai" University, Arany Janos Street, Number 11, Ro-400028, Cluj-Napoca, Romania

Received: June 1, 2010; Revised Manuscript Received: October 12, 2010

This study aims to present a detailed theoretical investigation of noncovalent intermolecular interactions between different $\pi-\pi$ stacking phenothiazine derivatives and between different alkane chains varying from propane to decane. Second-order Møller−Plesset perturbation (MP2), coupled cluster (CC), and density functional (DFT) theories were the quantum chemistry methods used in our calculation. For MP2 and CC methods, the density-fitting and local approximations were taken into account, while in the case of DFT, the M06 and M06-2x hybrid meta-GGA exchange-correlation functionals as well as the semiempirical correction to the DFT functional for dispersion (BLYP-D) was considered. The results obtained with the aforementioned methods were compared with the potential energy curve given by the DF-SCSN-LMP2 theory considered as benchmark. For all these calculations, the correlation-consistent basis sets of cc-pVNZ (where N = D, T, Q) were used. In addition, potential energy curves built using the semiempirical PM6-D2 and the MM3 molecular force field methods were also compared with the benchmark curve and their efficiency was discussed. As the next step, several geometry conformations were investigated for both phenothiazine derivatives and alkane chain dimers. It was found that the conformational stability of these molecular systems is exclusively given by the dispersion-type electron correlation effects. The density functional tight-binding (DFTB) method applied for dimer structures was compared with the results obtained by the higher level local perturbation theory method, and based on these conclusions larger phenothiazine derivative oligomers structures were investigated. Finally, the optimal configuration of the complex molecular systems built by phenothiazine derivative, alkane chain fragments, and thiol groups was determined, and their self-assembling properties were discussed.

1. Introduction

The controlled assembly of molecules is the key process for developing new nanostructured molecular materials with a wide range of applications in chemistry, biology, and medicine.[1−4] The structures and properties of these supramolecular systems are based on different types of intermolecular interactions, like hydrogen bonds (H bonds),[5] weak van der Waals (vdW) forces,[6] or charge-transfer complexes.[7] Attractive interactions between aromatic π systems are one of the main noncovalent VdW forces governing the supramolecular organization and recognition processes. These aromatic $\pi-\pi$ interactions are ubiquitous in diverse areas of science and molecular engineering.[8−11] They are one of the most important interactions in the vertical base stacking of DNA[12,13] and also could influence the tertiary structure of proteins.[14] Furthermore, $\pi-\pi$ interactions play a major role in stabilizing host−guest complexes[15,16] and in organic molecules self-assembling,[17−19] too.

In spite of the fact that parallel-displaced $\pi-\pi$ stacking interactions have been recognized to be an important force in stabilizing the double-helical structure of DNA and the tertiary structure of proteins, less features are known about their roles in self-assembled monolayers (SAM). SAMs are organic assemblies formed by the absorption of molecular constituents from solution or the gas phase onto the surface of solids or in irregular arrays on the surface of liquids where the adsorbents organize spontaneously (or induced[20]) into crystalline (or semicrystalline) structures or into different ordered forms. SAMs have four essential components which define their structure: the metal substrate, the ligand (or headgroup), the spacer (usually built by alkane chain), and the terminal functional group, where the last three components form a self-consistent molecular unit.[21] The matter of self-assembly can be characterized by the spontaneous and reversible organization of these molecular units into ordered structures by noncovalent interactions which occur between the spacer units as well as between the functional groups. The ligand−metal interaction reduces the large variety of association geometries contributing to the supramolecular ordering. Besides all that, the functional group has another important role: it defines the specificity of the fabricated SAM. It is the key ingredient which determines the linkage property between the SAM and the different functional molecular parts (like functionalized proteins, etc.). Accordingly, one of the most promising target classes of molecules is the aromatic thiol family.[22] In the class of aromatic thiols we are interested in several molecular species from the phenothiazine family which are potential candidates for establishing a strong $\pi-\pi$ stacking interaction. A detailed presentation of 3,7-dibromophenolthiazine derivatives, as a possible candidate for SAMs functional group, can be found in ref 23.

The phenothiazine (PTZ) derivatives have been selected due to their wide applicability. The PTZ molecule has been the basis for the development of antihistamines and antipsychotic drugs.[24] A theoretical investigation of their biological activity was

* To whom correspondence should be addressed. E-mail: bende@itim-cj.ro.

† National Institute for Research and Development of Isotopic and Molecular Technologies.

‡ "Babeş-Bolyai" University.

10.1021/jp105012g
Published on Web 11/04/2010

reported in ref 25. They are also basic dyes that possess redox properties and can be useful constituents in supramolecular assemblies[26] and components in photogalvanic systems for potential solar energy conversion.[27] PTZ and its derivatives are light sensitive, exhibit electron-donor properties, are used as chromophores for photoinduced electron transfer experiments,[28] and are a very promising candidate for new emissive and charge-transport materials for high-efficiency organic light-emitting diodes.[29] Possessing electron-donating substituents, this class of molecules maximally absorbs light within the biological therapeutic window (600−800 nm).

Due to their properties, PTZ derivatives are interesting candidates for obtaining new materials (e.g., via mercapto or thioacetate derivatives) by deposition as self-assembled monolayers (SAMs) on Au(111) surface. Some recent publications revealed special properties for the aggregates obtained by the deposition of phenothiazine units on gold nanoparticules via mercapto derivatives.[30] An exhaustive theoretical investigation of single-molecule PTZ derivative absorption on Au(111) surface was presented by Morari et al.[31] They have shown that the interaction energy between the Au(111) surface and the PTZ derivative molecule with 6 different relative positions is ranking between 48.4 and 78.4 kcal/mol.

The goal of this study is to make the first step toward modeling the self-assembling properties for different oligomer structures of the phenothiazine molecule and its derivatives. More precisely, our contribution focuses on the detailed description of the energetic aspects of the molecular self-association. Accordingly, after an adequate description of the applied methods (section 2), we present in detail the nature of noncovalent intermolecular interaction for several dimer conformations of phenothiazine and alkane chains using different theoretical methods (section 3). After validation of the tight-binding density functional method by comparing it with higher level theoretical methods, in the same section we present larger oligomer structures formed by phenothiazine and alkane fragments. Finally, pathways connecting all these effects on the self-assembling properties of phenothiazine derivatives are discussed in section 4, and our conclusions are presented in section 5.

2. Methods

Noncovalent interactions of aromatic $\pi-\pi$ complexes are mainly determined by a complicated interplay between vdW (also called dispersion) and electrostatic (ES) interactions.[32−35] At short intermolecular distances, exchange-repulsion (EXR) contributions (which derive from the Pauli principle) dominate the interactions. The ES and EXR contributions can already be described accurately at the Hartree−Fock (HF) level of theory, whereas dispersion interactions represent pure electron correlation effects.[36] According to Grimme's investigation[37] on different polycyclic aromatic hydrocarbons as well as on different polycyclic saturated hydrocarbons, some refinement must be taken into account regarding the "$\pi-\pi$" interaction term. He suggests using this term in the discussion of noncovalent binding between neutral closed-shell systems with care because for systems with about 10 carbon atoms or less there is little theoretical evidence for a special role of the π orbitals. Thus, hereafter we will use the term "$\pi-\pi$" stacking as a geometrical descriptor of the interaction mode in unsaturated molecular systems and as a special type of electron correlation (dispersion) effect in the stacked orientation.

The widely used exchange-correlation functionals, defined in the framework of Kohn−Sham (KS) density functional theory (DFT), treat the electron correlation only in an approximate manner, without including dispersion effects (e.g., see refs 38−40 and references therein). On the other hand, it is also established that second-order Møller−Plesset (MP2) perturbation theory tends to slightly overestimate the intermolecular interaction energies and to underestimate intermolecular distances[41−43] as well. More sophisticated methods based on coupled-cluster theory (e.g., CCSD(T) coupled cluster with single, double, and perturbative triple excitations) are computationally very expensive (or in most cases unfeasible) with reasonably large basis sets already for medium size systems.[36] Nevertheless, in order to obtain sufficiently accurate intermolecular interaction energies or bond distances, one needs to include successively larger shells of polarization (correlating) functions and diffuse functions, respectively, in our basis sets. In addition, these energy values and distances also have to be corrected by excluding the basis set superposition errors (BSSE),[44,45] which could distort the results very much.[46] Recently, a large number of theoretical studies broach the problem of long-range electron correlation effects. Most of them can be classified in several major directions: (1) The first direction is based on the range-separated hybrid (RSH) approach introduced in the generalized KS formalism, where long-range exchange and correlation effects are treated by wave function methods (e.g., second-order perturbational corrections), while short-range electron exchange and correlation are handled by local or semilocal exchange-correlation (XC) functionals.[47−50] (2) The second major direction consists in applying empirically corrected XC functionals by dispersion effects, where the classical DFT energy is incremented by a semiempirically parametrized, damped $1/R^6$ energy term.[51,52] (3) Having the same idea of improving the XC functionals, the next direction is based on the concept of atom-centered effective core-type potentials.[53,54] These dispersion-correcting potentials (DCPs) correct the erroneous long-range behavior of DFTs by changing the potentials in which the electrons move such that the correct dispersion binding behavior is approximated. In this way, the deviations of total DFT energies of interaction from MP2 results was drastically reduced. The method was successfully tested against the S22[55] benchmark set containing noncovalently bound complexes,[56] and it was applied in the case of medium- and large-size molecular systems as large, polyaromatic hydrocarbon dimers[57] and thiophene and benzothiophene dimers.[58] (4) The fourth direction consider studies which include the highly parametrized hybrid meta-GGA XC functionals (e.g., the M06 or M06-2x XC functionals,[59] and references therein, developed by the Truhlar group), where, based on the database of the results obtained with high correlation methods and large basis sets, the parametrization of XC functionals are extended also for the vdW region. (5) While the methods presented in the first four cases are derived from the KS formalism, the last one is based on classical Møller−Plesset perturbation or coupled-cluster (CC) theory but using localized orbitals instead of canonical ones.[60] For the computation of intermolecular interactions, local electron correlation methods[60−62] have been proven to give values which are very close to the standard MP2 results and by construction they are virtually free of BSSE.[61,62] Linear scaling of the computational cost as a function of the system size[63] makes it possible to treat larger systems or to use larger basis sets. Using the density-fitting (DF) approximation of the electron repulsion integrals[64−66] one can reduce again the computation time by about 1 order of magnitude, applying it in both HF and LMP2 cases (DF-HF and DFLMP2). In particular, the efficiency of DF-LMP2 method in describing the π-stacked intermolecular interaction in the case of benzene dimer structures dominated by the dispersion forces

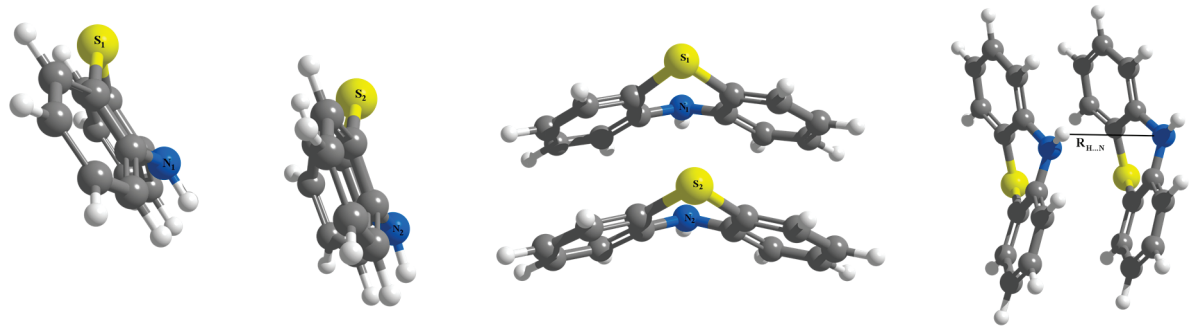

Figure 1. Geometry structure of PTZ dimer obtained at DF-HF (a) and DF-LMP2 (b and c) levels of theory.

was clearly demonstrated by Hill et al.[67] In this way, the computational cost where in the case of the second-order Møller−Plesset perturbation theory (MP2) scales formally with $O(N^5)$ is reduced to $O(N)-O(N^2)$ without losing much of the accuracy of our calculations.

Due to the computer capacity limits, theoretical methods presented in the previous paragraph together with middle large basis sets are capable of handling molecular systems with approximately 150 atoms. At the same time, in the self-assembling processes are involved molecular systems, which all together contain more than 200−300 atoms. The density functional-based tight-binding method combined with the self-consistent charge technique (SCC-DFTB)[68] can be considered as an adequate solution for treating large biologically interested or nanoscaled molecular materials with nearly good accuracy as obtained in the case of high-level theoretical methods.[69−71] An empirical dispersion correction has also been developed, and it was found to be crucial for predicting reliable nucleic acid base stacking interactions,[71] the relative stability of α and 3_{10} helices in proteins,[72] and the stability of the double-stranded DNA tetramer with a ligand in the intercalative fashion.[73]

Using the DF-LMP2 method implemented in the Molpro program package suite,[74] we performed geometry optimization for different dimer conformations of PT and its derivatives as well as for different C_nH_{2n+2} alkane chains ($n = 3-10$), using the cc-pVNZ (N = D, T)[75,76] basis sets. Taking the program parameter descriptions as presented in refs 67 and 77 we used the following input settings: (i) instead of the Pipek−Mezey localization procedure[78] we considered the natural localized molecular orbitals (NLMO),[77] since NLMOs are much less sensitive to the basis set, in particular when diffuse functions are used; (ii) in order to solve an occurrent poor orbital localization in the NLMO technique when the larger diffuse basis set were used, we eliminate the contribution of the diffuse basis functions to the localization criteria by setting the corresponding rows and columns of the overlap matrix used in the NLMO localization to zero; (iii) the domains of the three aromatic π orbitals in each benzene-type ring were merged, leading to the three identical domains that include the p_π atomic orbitals of all 6 carbon atoms from the given six-membered ring. Considering the local character of occupied and virtual orbitals in the local correlation treatment, one can easily obtain also the dispersion part (an intermolecular effect) of the correlation contribution.[79] The intermolecular potential energy curves for PTZ dimer were computed using different basis sets cc-pVNZ (N = D, T, Q) with and without augmented diffuse functions] and different theoretical models. Accordingly, the recently introduced Truhlars M06-2x and the dispersion-corrected BLYP-D results were compared with the density-fitting HF as well as with the density-fitting local correlation [DF-LMP2 and DF-LCCSD(T)] methods, where the M06, M06-2x, and DFT-D (considering the BLYP-D XC functional with empirical dispersion corrections) energy values were obtained using the NWChem program package.[80] In order to extend our study for larger PTZ molecular clusters, the intermolecular potential energy curve obtained with the DF-LMP2 method together with cc-pVTZ basis set was also compared with the similar potential curve drawn by applying the density functional tight-binding (DFTB)[81,82] method with dispersion correction.[70] Molecular structures were visualized and analyzed using the Gabedit[83] molecular graphics program.

3. Results and Discussions

3.1. Phenothiazine Dimer. The phenothiazine molecule is built up by two aromatic benzene rings, linked by two bridges of nitrogen and sulfur atoms, where the planes of benzene rings form an angle close to 135°. The geometry optimization procedure of the PTZ dimer was started taking different arbitrary initial positions and considering the DF-LMP2 theoretical methods together with the cc-pVDZ (*vdz*) basis set. In order to improve the quality of the applied basis set, the geometry optimization was repeated taking the previous geometry structure but considering the cc-pVTZ (*vtz*) basis set. All these geometry optimization calculations were performed also in the case of the HF level. From several dimer conformations obtained with the DF-LMP2 method with *vdz* basis set, the "V stacking" (VS) configuration (Figure 1a, 1b, and 1c) has been found as the energetically most stable geometry structure. Accordingly, in Figure 1a we present the dimer geometry obtained with DF-HF method, while in Figure 1b and 1c the DF-LMP2 geometry together with different geometry parameters and characteristic atoms are shown. These geometrical parameters as well as intermolecular energies and their dispersion components for the correlated case are collected in Table 1.

Comparing the intermolecular distances between nitrogen ($d^{N_1\cdots N_2}$) and sulfur ($d^{S_1\cdots S_2}$) atoms, a large deviation between the DF-HF and the DF-LMP2 geometries was observed (from the value of 5.25 Å obtained at the DF-HF/*vdz* method the $d^{N_1\cdots N_2}$ distance decreases to 3.75 Å at the DF-MP2/*vdz* level, while the $d^{S_1\cdots S_2}$ distance becomes shorter with 1.94 Å). The HF/*vtz* geometry optimization gives the same dimer form as it was found in HF/*vdz* case. Here, the intermolecular distances are $d^{N_1\cdots N_2} = 5.54$ Å and $d^{S_1\cdots S_2} = 6.30$ Å. These geometry discrepancies prove that electron correlation effects play an important role in the stability of the dimer structures. These findings are also confirmed by the intermolecular interaction energy values obtained at the HF and correlation levels. Namely, it can be observed that only the correlation case shows a stable

TABLE 1: Different Geometry and Energy Parameters of the PTZ Dimer Geometries Obtained at the DF-HF and DF-LMP2 Levels of Theory, Using the cc-pVDZ and cc-pVTZ Basis Sets

	basis set	
geometry parameters	cc-pVDZ	cc-pVTZ
DF-HF		
ΔE_{HF} [kcal/mol]	−0.6	−0.9
$d^{N_1...N_2}$ [Å]	5.3	5.5
$d^{S_1...S_2}$ [Å]	5.9	6.3
DF-LMP2		
ΔE_{HF} [kcal/mol]	+7.6	+11.8
ΔE_{LMP2} [kcal/mol]	−7.6	−11.6
ΔE_{corr} [kcal/mol]	−15.2	−23.4
ΔE_{disp} [kcal/mol]	−12.7	−18.7
$d^{N_1\cdots N_2}$ [Å]	3.75	3.66
$d^{S_1\cdots S_2}$ [Å]	3.92	3.83

structure having a well-defined bounding energy (ΔE_{LMP2} = −7.6 kcal/mol), while the DF-HF/*vdz* optimized configuration can be considered as an unbounded system, having a very small bond energy (ΔE_{HF} (*vdz*) = −0.6 kcal/mol) and large intermolecular equilibrium distance. Hereafter we use the notation "Δ" for the intermolecular interaction energy as well as for its components.The same behavior can be said for the DF-HF/*vtz* case, where ΔE_{HF}(*vtz*) = −0.9 kcal/mol. If one considers only the correlation case, the contrast between HF and correlation levels is more stressed. While for the DF-LMP2/*vdz* geometry the HF component (ΔE_{HF}) of the interaction energy shows a large positive value (+7.7 kcal/mol) giving a repulsion character for this interaction, the geometry is expressly stabilized by the electron correlation (defined as the difference of the intermolecular interaction energies obtained at the correlation and HF levels) effects (ΔE_{corr} = −15.3 kcal/mol), where the most important contribution is given by the dispersion-type correlation (ΔE_{disp} = −12.7 kcal/mol). In the case of the DF-LMP2/*vtz* geometry, the HF component is +11.8 kcal/mol, the total electron correlation energy has a value of −23.4 kcal/mol, while the dispersion-type correlation energy is −18.7 kcal/mol.

Furthermore, analyzing the effects which occur when we apply different basis sets in the geometry optimization, some important conclusions can be stated. First, the changes in energies like HF, total correlation, and dispersion energies are much stronger that those for the equilibrium geometry. More exactly, the changes in $d^{N_1\cdots N_2}$ and $d^{S_1\cdots S_2}$ intermolecular distances are around ∼0.1 Å, which with a good approximation can be considered as a small basis set effect on the geometrical parameters. However, this is not the case for the energies, where we have a 4−6 kcal/mol energy increase on average for all kinds of energy values. It can be observed that when we increase the dimension of the basis set, both the repulsive contribution of the HF level (from +7.7 to +11.8 kcal/mol) and the attractive part given by the electron correlation (from −15.3 to −23.4 kcal/mol) increase in absolute value in such a way that the resulting total intermolecular interaction energy will also increase in its absolute value (from −7.6 to −11.6 kcal/mol). This conclusion is telling us that correlation effects are more sensible on the dimension of the basis set than those obtained at the HF level.

In order to explore in more detail how the basis set quality influences different energy components, we performed several single-point energy calculations considering the DF-LMP2/*vtz* geometry and using a wide range of cc-pVNZ (where N = D,T,Q) and aug-cc-pVNZ (where N = D,T) basis sets. The corresponding results are presented in Table 2. For smaller basis

TABLE 2: Intermolecular Interaction Energies and Dispersion Energy Components of the PTZ Dimer Obtained at DF-HF, DF-LMP2, and DF-LCCSD(T) Levels of Theory, Using the cc-pVDZ (*vdz*), cc-pVTZ (*vtz*), cc-pVQZ (*vqz*), aug-cc-pVDZ (*avdz*), and aug-cc-pVTZ (*avtz*) Basis Sets[a]

method	basis set	ΔE_{HF} [kcal/mol]	ΔE_{LMP2} [kcal/mol]	ΔE_{disp} [kcal/mol]
DF-LMP2	*vdz*	+9.7	−8.7	−14.4
	vtz	+11.8	−11.6[b]	−18.7
	vqz	+12.6	−13.2	−20.4
	avdz	+8.7	−14.2	−20.5
	avtz	+12.3	−14.9	−21.6

[a] For all these energy calculations the DF-LMP2/*vtz*-optimized geometry has been used. [b] $\Delta E_{LCCSD(T)}$ = −11.177 kcal/mol.

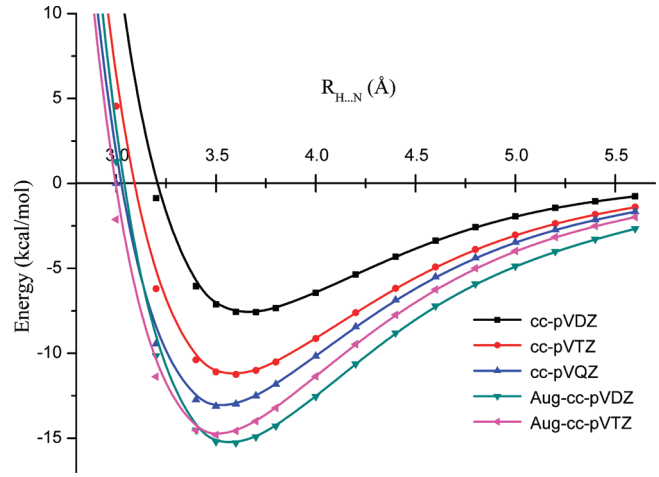

Figure 2. DF-LMP2 intermolecular potential energy curves obtained along the $R_{H\cdots N}$ intermolecular distance (see Figure 1c) considering the cc-pVDZ, cc-pVTZ, cc-pVQZ, aug-cc-pVDZ, and aug-cc-pVTZ basis sets.

sets, i.e., cc-pVDZ (*vdz*), cc-pVTZ (*vtz*), and aug-cc-pVDZ (*avdz*), the ΔE_{HF} HF energy component shows an irregular behavior, while for a larger basis set like cc-pVTZ, aug-cc-pVTZ (*avtz*), and cc-pVQZ (*vqz*) a saturation effect was observed. A much clearer basis set dependency was found in the case of the ΔE_{disp} dispersion-type component of the correlation energy. If one considers basis sets without augmented basis functions, the dispersion energy increasing was still significant (the dispersion energy difference between *vdz* and *vtz* values is 4.3 kcal/mol and between *vtz* and *vqz* is 1.7 kcal/mol), while if the augmented basis sets were included in the energy calculations, the difference between the results obtained for two consecutive basis sets was smaller (the dispersion energy difference between *avdz* and *avtz* values is 1.0 kcal/mol). The ΔE_{LMP2} total interaction energy which includes both the HF and MP2 contributions shows nearly the same tendency as that found in the case of dispersion-type correlation energies. Accordingly, the intermolecular potential energy curves obtained along the $R_{H\cdots N}$ intermolecular distance parameter (see Figure 1c) considering the *vdz*, *vtz*, *vqz*, *avdz*, and *avtz* basis sets are presented in Figure 2. These results conclude that if one wants to describe accurately the intermolecular interaction in the PTZ dimer, at least the MP2 level of theory should be considered together with *avdz* or *avtz* basis sets.

In spite of the fact that the local correlation treatment combined with the density-fitting technique can, in general, provide calculations with much lower computational costs, the deficiency of the standard MP2 theory (overestimates the dispersion forces in π-stacked systems) remains also an attendant

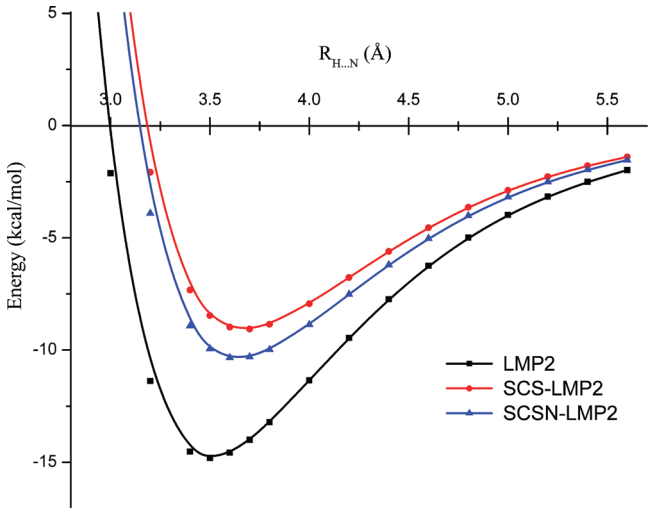

Figure 3. Intermolecular potential energy curves obtained along the $R_{H\cdots N}$ intermolecular distance (see Figure 1c) considering the DF-LMP2, DF-SCS-LMP2, and DF-SCSN-LMP2 theoretical methods with the aug-cc-pVTZ basis set.

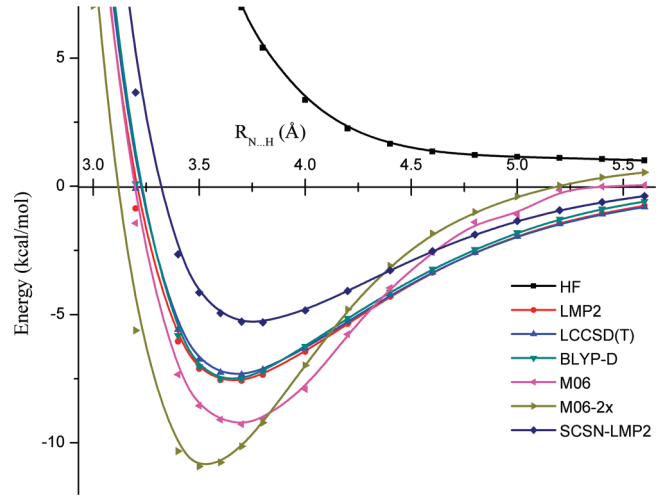

Figure 4. Intermolecular potential energy curves obtained along the $R_{H\cdots N}$ intermolecular distance (see Figure 1c) considering the DF-HF, DF-LMP2, DF-LCCSD(T), BLYP-D, M06, M06-2x, and DF-SCSN-LMP2 (benchmark) theoretical methods with cc-pVDZ basis sets.

of the LMP2 method. Hill et al.[67] performed a detailed theoretical investigation for different dimer configurations of benzene, and they found that the LMP2 results are quite far from the counterpoise-corrected CCSD(T) values. For example, the interaction energy in the parallel-displaced benzene dimer is −4.0 kcal/mol for LMP2/*avtz** and only −2.5 kcal/mol in the case of CCSD(T)/*avtz** (avtz* = aug-cc-pVTZ for C atoms and cc-pVTZ for H atoms). At the same time, if they applied the so-called spin-component scaled (SCS) MP2 theory[84] (for both canonical and localized orbitals) the discrepancy was small compared with the CCSD(T) results. However, in their later work[85] they showed that in the case of stacked nucleic acid systems the SCS-LMP2 method fails to describe correctly the intermolecular interaction energies, where its mean deviation from the best estimated values of the S22 set[55] is −1.62 kcal/mol. Accordingly, instead of the default scaling factor of 6/5 for antiparallel spins and 1/3 for parallel spins they completely neglect the contribution from antiparallel-spin electron pairs to the MP2 energy and scaled the parallel contribution by 1.76. In this way, they obtained a mean deviation of −0.04 kcal/mol. The method is called spin-component scaled LMP2 for nucleobases (SCSN-LMP2). Choosing the spin-component scaling factors empirically, they accentuated that the methodology can no longer be considered a truly ab initio method but provides a substantial correction to the MP2 overestimation of the dispersion energy at no extra cost. The potential curves obtained with DF-LMP2, DF-SCS-LMP2, and DF-SCSN-LMP2 by using the *avtz* basis set are presented in Figure 3, taking the optimized geometry of DF-LMP2/*vtz*. Setting against the potential energy profiles one can see that the DF-LMP2 method has about 4.4 kcal/mol deeper minima than the DF-SCSN-LMP2 one, while Grimme's DF-SCS-LMP2 method has a weaker bounding with about 1.3 kcal/mol if one compares with the same DF-SCSN-LMP2 method. Summarizing the results presented, we emphasize two important energy values for further comparisons. The first is obtained using the DF-LMP2 method with the *avtz* basis set and will be the reference energy for the *functional group* from the SAM units ($\Delta E_{LMP2} = -14.8$ kcal/mol). The second one is calculated using the DF-SCSN-LMP2 theory with the same *avtz* basis set and having a more realistic value for the intermolecular interaction energy in the PTZ dimer ($\Delta E_{SCSN-LMP2} = -10.4$ kcal/mol), which we consider as the benchmark potential energy curve for other theoretical methods.

After an exhaustive analysis of basis set dependency on the intermolecular interaction energy and bond distance, a similar investigation was performed on theoretical methods other than the perturbational one. Accordingly, we compared the DF-LMP2 results with those obtained by HF, CC, and three DFT methods including the BLYP-D, M06, and M06-2x XC functionals. In all cases, only the *vdz* basis set was considered. Selection of this basis set is imposed by the computer capacity limit in calculating the DF-LCCSD(T) energy, considered by us as the reference energy. The results are presented in Figure 4. Due to the lack of the electron correlation at the HF level, the corresponding potential energy curve shows an unbounded behavior. At first sight, this is slightly contradictory with the HF results presented in the first part of this section, where we obtained a small negative value ($\Delta E_{HF} = -0.6$ kcal/mol), but one should not forget that the chosen intermolecular direction along the dimer system was moved far from the optimized HF geometry. Comparing the DF-LMP2 and DF-LCCSD(T) potential curves, no large discrepancies can be found between these methods. This means that most of the electron correlation is covered by the MP2 approximation at the *vdz* basis set level. Similar good agreement can be observed in the case of DF-LMP2 and BLYP-D results. Practically, there are no differences between the second-order local correlation potential curve and the values obtained with the empirically corrected DFT by dispersion (BLYP-D). Inspecting the potential energy profiles obtained with M06 and M06-2x hybrid meta-GGA XC functionals and comparing them with the DF-LMP2 values, one can see that the first two potential energy curves show larger potential minima than the last one. The difference between M06 and DF-LMP2 values is 1.7 kcal/mol, while between M06-2x and DF-LMP2 it is 3.3 kcal/mol. Moreover, their asymptotical behavior shows a wrong dependency, giving positive values for the intermolecular interaction energy at large intermolecular distances (>5.1 Å). It can also be observed that the M06-2xs asymptotical limit is closer to the positive values of the HF profile than to the zero limit of negative energy region. One should mention that the M06-2x functional contains 54% of the HF exchange by construction, while the M06 contains only 27%. This suggests that at large intermolecular distance, the HF exchange contribution from the M06-2x XC functional gives an excessive repulsion effect, which is not counterbalanced by the correct dispersion attraction. A very comprehensive work

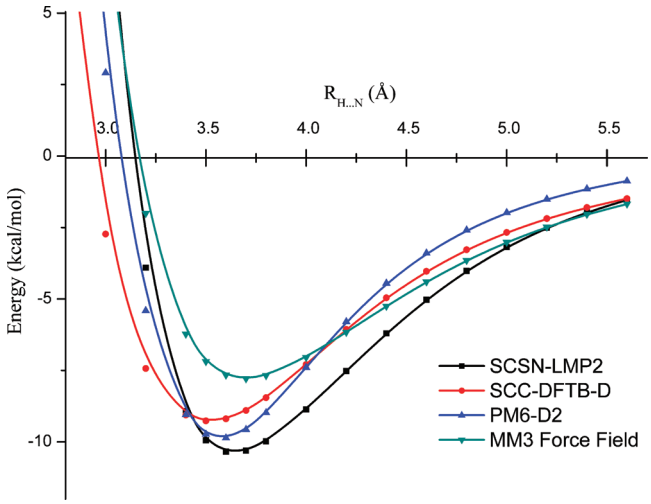

Figure 5. Intermolecular potential energy curves obtained along the $R_{H\cdots N}$ intermolecular distance (see Figure 1c) obtained at the DF-SCSN-LMP2 level with aug-cc-pVTZ basis sets as well as at the SCC-DFTB-D, semiempirical PM6-D2, and MM3 force field levels of theory.

of Johnson et al.[86] and Mackie et al.[87] shed light on the different problems which could occur in the case of meta-GGA XC functionals when we try to describe dispersion-bounded complexes. According to them, these could manifest as the potential energy oscillate behavior because of the quality of the chosen grid or as the poor description of the far intermolecular region. Similar conclusions were drawn by Hohenstein et al.,[88] where they point out that the dispersion interaction is not really captured by the M06-2x functional (included in its correlation functional part) at the long-range intermolecular separation. Considering the benchmark potential energy curve obtained with the DF-SCSN-LMP2 method and comparing it with the DF-LCCSD(T) results one can observe that the intermolecular interaction energy for the equilibrium geometry obtained with the DF-LCCSD(T) method is larger at 1.85 kcal/mol. At the same time, one should emphasized that in the case of benzene aromatic rings, no direct calculation was found in the literature where the DF-SCSN-LMP2 and DF-LCCSD(T) methods were explicitly compared.

In the previous section we concluded that different DFT functionals where the dispersion corrections were taken into account can be described more or less correctly by the $\pi-\pi$ stacking intermolecular interaction in the PTZ dimers. However, similar to the local perturbational methods, they are not able to handle larger clusters or even self-assembled structures. The density functional-based tight-binding method together with self-consistent charge technique (SCC-DFTB) and empirical dispersion correction could offer us a suitable framework to handle properly these large molecular clusters. As the first step, one has to test the SCC-DFTB-D method in order to make sure of its efficiency. Accordingly, the intermolecular potential energy curve for PTZ dimer obtained with the SCC-DFTB-D method were compared with a similar energy curve calculated by the DF-SCSN-LMP2 method using the *avtz* basis set (Figure 5). The results show that the long-range part of the SCC-DFTB-D curves (blue color with inverse triangle) dominated by the empirical dispersion correction is close to the DF-SCSN-LMP2/*avtz* potential energy curve, while the short-range repulsive part is less ascendant than the local-MP2 curves. The minimum energy of the SCC-DFTB-D potential is weaker with about 1.0 kcal/mol, while the equilibrium intermolecular bond distance is very close to the DF-LMP2/*avtz* value (~3.5 Å). At the same time, a small discrepancy can be observed in the angle defined by the plane of the benzene rings, compared with the DF-LMP2 result. While the local-MP2 method has an angle of 135°, the SCC-DFTB-D method gives a larger value with about 13° (~148°). This relatively good agreement between SCC-DFTB-D and local MP2 results shows that large systems which contain all three (*functional group*, *spacer*, and *linker*) components could be described with the same accuracy as that obtained for the PTZ dimer.

In the last decay remarkable progress also has been obtained in the efficient parametrization of different molecular force fields and semiempirical methods. An exhaustive theoretical investigation was presented by Sherrill et al.,[89] where several popular force fields have been tested for their ability to reproduce highly accurate quantum mechanical potential energy curves for noncovalent $\pi-\pi$ stacking interactions. They conclude that, in general, all of the used force field methods can qualitative correctly describe the noncovalent $\pi-\pi$ stacking interactions but are not able to consistently reproduce the benchmark potentials obtained at the ab initio level, and their performance is not consistent from one chemical system to the next. At the same time, the Hobza group[90,91] improved the quality of the PM6[92] semiempirical method by adding empirical dispersion correction and successfully applied the method in the case of large molecules with biological relevance, showing that the quality of current DFT-D approaches for these types of problems can be reached also by the PM6-DH2 method. Accordingly, in Figure 5 we also present the potential energy curve obtained by the PM6-D2 method using the MOPAC software[93] and the curve calculated with the MM3 force field[94] using the TINKER molecular modeling package,[95−97] respectively. We observed that for the potential curves minima the PM6-D2 method gives the best approach compared to the ab initio method (even better than the SCC-DFTB-D), but its long-range behavior is far from the same reference curve (underestimated by ~0.7 kcal/mol). On the other hand, the MM3 generation force field method gives correct short-range and long-range behaviors but the worst approach for the curve's minima (underestimated by ~2.5 kcal/mol).

3.2. Dimers of Phenothiazine Derivatives. In order to study in a more realistic form, but on the other hand to maintain the proper theoretical level of our description, we considered six different dimer configurations of ethyl-phenothiazine (EPT), where the N−H bond of the PTZ molecule was substituted by an ethyl group (see Figure 6). Accordingly, the EPT dimer structure geometries were optimized considering the DF-LMP2/*vdz* level of theory, while the intermolecular interaction energy and its dispersion part were obtained at the DF-LMP2/*vtz* theoretical level. In our preliminary work[98] we already presented the parallel (EPT-C2) and antiparallel (EPT-C3) stacking dimers by comparing the intermolecular interaction energies obtained with DF-HF/*vdz* and DF-LMP2/*vdz* methods. Since then, four dimer configurations (EPT-C1, EPT-C4, EPT-C5, and EPT-C6) have been included in our investigation. All six dimer geometries are shown in Figure 6, ranking from the lowest total energy configuration (EPT-C1) to the highest one (EPT-C6). For their characteristic energies see Table 3. The energy difference between the most and the less bounded conformations is 2.961 kcal/mol, while the difference between two successive geometry structures is in the energy interval of 0.6−1.0 kcal/mol, comparable with the *thermal energy* of a molecule at *room temperature* (for $T = 298$ K it is 0.6 kcal/mol). An exception is the case of EPT-C5 and EPT-C6 geometries, where we obtained only a difference of 0.085 kcal/mol. In the most stable

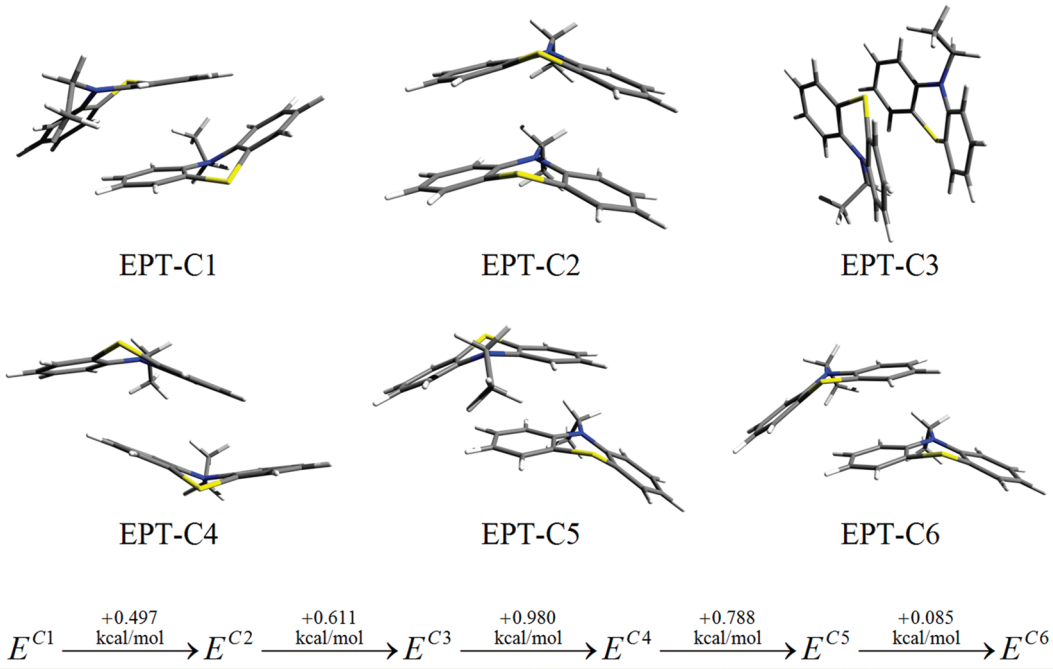

Figure 6. Conformational structures and their relative conformational energies for different ethyl-phenothiazine (EPT) dimers obtained at the DF-LMP2/cc-pVTZ level of theory.

TABLE 3: Intermolecular Interaction Energies and the Dispersion Energy Parts of Six EPT Dimer Configurations Obtained at DF-HF and DF-LMP2 Levels of Theory, Using the cc-pVTZ (*vtz*) Basis Set

conformation	ΔE_{HF} [kcal/mol]	ΔE_{LMP2} [kcal/mol]	ΔE_{corr} [kcal/mol]	ΔE_{disp} [kcal/mol]
EPT-C1	+7.3	−13.9	−21.2	−18.1
EPT-C2	+9.3	−13.7	−23.1	−18.8
EPT-C3	+9.5	−12.6	−22.1	−19.1
EPT-C4	+6.9	−11.7	−18.6	−15.9
EPT-C5	+5.7	−11.0	−16.7	−14.4
EPT-C6	+6.7	−10.4	−17.1	−14.6

configuration (EPT-C1) the "V" shapes of PTZ molecular fragments are facing each other, while the ethyl groups are sitting in the opposite direction. This conformation is characterized by an optimal balance between the repulsive electrostatic energy (ΔE_{HF} = +7.3 kcal/mol) and the attractive electron correlation energy (ΔE_{corr} = −21.2 kcal/mol), yielding the most stable dimer structure with the strongest intermolecular interaction energy (ΔE_{LMP2} = −13.9 kcal/mol). Concerning the PTZ fragment, the second (EPT-C2) and third (EPT-C3) structures having the "V stacking" form, the difference is in the relative positions of the ethyl groups. They show large repulsive HF energy components (+9.3 and +9.5 kcal/mol·s) as well as large electron correlation contributions (−23.1 and −22.1 kcal/mol·s) mostly covered by the dispersion effects (−18.8 and −19.1 kcal/mol·s). The last two weakly bounded dimer structures contain semi-"V-Stacking" PTZ fragments with ethyl groups in two different positions. These relative shifts of the benzene rings give smaller electrostatic repulsion (+5.8 and +6.7 kcal/mol·s) as well as smaller electron correlation effects (−16.7 and −17.1 kcal/mol·s). One of the most important characteristics of these dimer conformations is how they could turn over from a certain conformation to the other one. In this way, we believe that conformational transitions can easily take place between the EPT-C2 and the EPT-C6 as well as between the EPT-C3 and the EPT-C5 dimer configurations by a simple shift of the benzene rings. These presumed geometry transformations show a value of +2.5 kcal/mol transition energy in the first case (from EPT-C2 to EPT-C6) and +1.8 kcal/mol for the second one. Furthermore, another dimer configuration was assembled, where one of the PTZ fragments stays perpendicular to the inner surface of the second PTZ fragment. Geometry optimization shows that the perpendicular (or the so-called "T-shape") configuration is not a stable structure; it turns over to one of the "V-Stacking" conformations: EPT-C2 or EPT-C3. Similar results were obtained by Mackie et al.[58] for dibenzothiphene. These six geometries investigated in this section were chosen after a detailed analysis of several EPT dimer-optimized configurations. We kept only those structures we considered to be relevant for the self-organization (showing high affinity for self-assembling). Accordingly, we considered all the structures where inside the PTZ dimer the double aromatic rings interact with each other (EPT-C1, EPT-C2, EPT-C3, EPT-C4), regardless of the ethyl group orientation. It can be seen that while in cases of EPT-C1 and EPT-C4 the parallel shift gives identical structures, for the EPT-C2 and EPT-C3 configurations we obtain different dimers (EPT-5 and EPT-6).

3.3. Alkane Chains. From the point of view of the self-assembling phenomenon, we consider the EPT-C2 configuration as the most suitable system. As we pointed out in the previous subsection, the conformational energy difference between EPT-C2 and EPT-C3 dimer structures is around 0.6 kcal/mol. Both geometries are stabilized by the interaction of the PTZ fragments. The difference in their stabilization energy is given by the position of ethyl groups and implicitly by their energy surplus due to their interactions. Hence, the role of a longer alkyl chain on the magnitude of the intermolecular interaction energy is important to be investigated in more detail. Using the conventional MP2 and CCSD(T) methods, the nature of the intermolecular interaction between different *n*-alkane dimers (from methane to decane) was investigated by Tsuzuki et al.[99,100] In their first paper, five different alkane dimer conformations were analyzed, while in the second work the most stable dimer was studied in more detail considering the high-level correlation method at the basis set limit. From our point of view, the top-

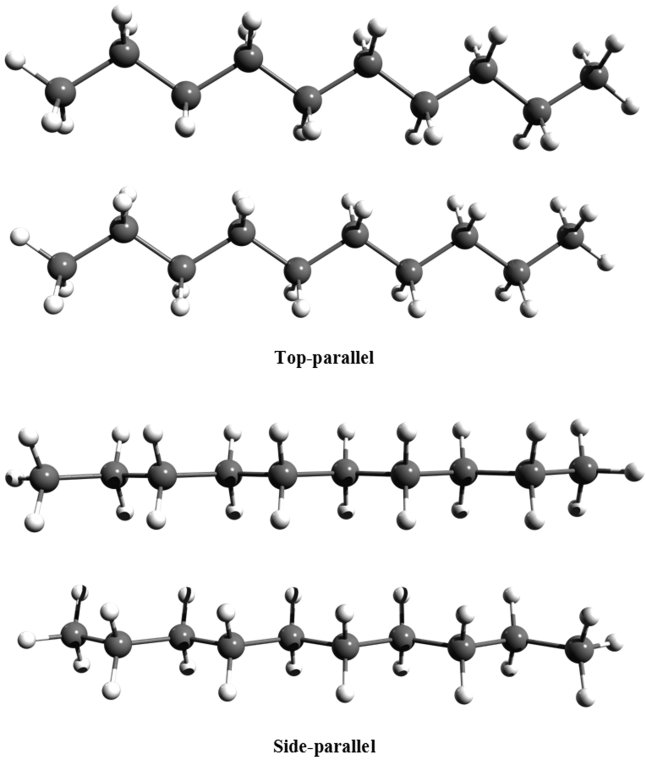

Figure 7. "Top-parallel" and "side-parallel" dimer conformations of the decane dimer.

parallel (where one of the zigzag alkane chains is at the top side of the other one) and side-parallel (where one of the zigzag alkane chains is at the side of the other one but rotated 180° along the chain axis) conformations are the major interest of our investigation. The two conformations of decane are shown Figure 7. The top-parallel conformation is characteristic of EPT-C2, while the side-parallel form is specific for the EPT-C6 conformation but only for a sufficiently long alkyl fragment. Accordingly, the structures of *n*-alkane dimer (from propane to decane) geometries were optimized considering the DF-LMP2 method and using the *avtz* basis set. The intermolecular interaction energies as a function of the alkane chains dimension for both top-parallel and side-parallel conformations are presented in Figures 8 and 9. The stability of the saturated hydrocarbons is given by the simple balancing of the repulsive electrostatic and attractive dispersion forces. Analyzing the size dependence of different energy components as we increase the alkane chain by adding a new methylene unit, one can find a linear behavior ($a + bN$, where $N = 1$ for methane, 2 for ethane, etc.) for both electrostatic and dispersion components as well as for the DF-LMP2 interaction energy. This linear behavior was already reported by Tsuzuki et al.[99,100] Linear dependencies which describe the intermolecular interaction energy are given by the following formulas: $E(N) = 0.343 - 0.445N$ for the top-side parallel configuration and $E(N) = 0.743 - 0.845N$ for the side-parallel conformation, where the constants are given in kcal/mol. Other linear dependencies which describe separately the repulsive (its HF contributions) and attractive dispersion (the dominant part of the electron correlation energy) energy components are explicitly shown in Figures 8 and 9. Comparing the linear dependencies which correspond to DF-LMP2 intermolecular interaction energies, one can see that the side-parallel intermolecular interaction is considerably stronger than that for the top-parallel case. The energy difference between the side-parallel and top-parallel conformations of decane is around 3.6 kcal/mol.

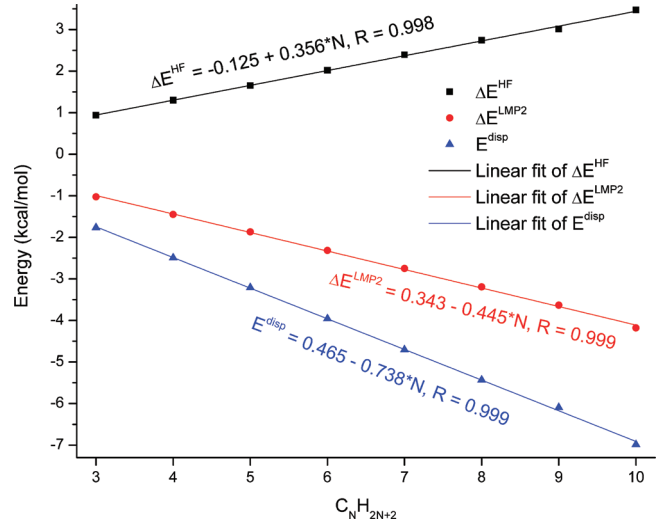

Figure 8. Intermolecular interaction energy of the "top-parallel" conformation of *n*-alkane dimers (from propane to decane).

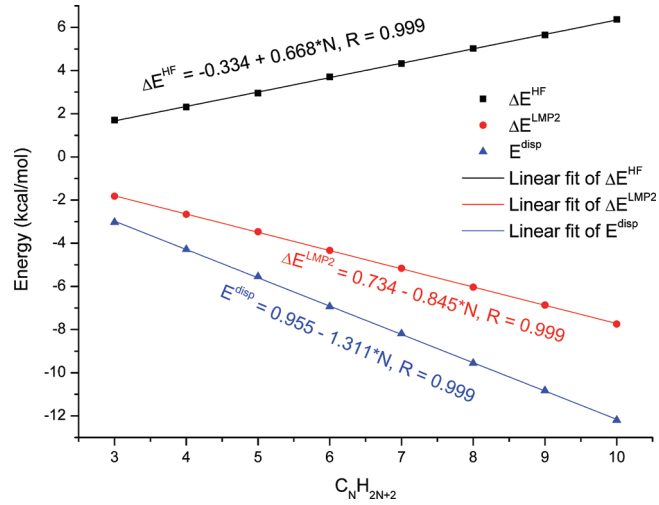

Figure 9. Intermolecular interaction energy of the "side-parallel" conformation of *n*-alkane dimers (from propane to decane).

3.4. SCC-DFTB Results. In order to obtain a comprehensive picture of the self-assembling process, one needs to treat the *functional group* (PTZ fragment), *spacer* (alkane chain), and *linker* (thiol group) all together and should also consider a suitable large number of monomers, requirements which could easily exceed the efficiency limit of any conventional ab initio method (HF, MP2, DFT, etc.).

In order to investigate the self-assembly properties of these structures we built several dimers and pentamers for different molecular species: hexyl-PTZ (*PTZ* + *hexane alkyl chain*), thio-pentyl-PTZ (*PTZ* + *pentane alkyl chain* + *SH*), decyl-PTZ (*PTZ* + *decane alkyl chain*), and thio-nonyl-PTZ (*PTZ* + *nonane alkyl chain* + *SH*), considering the SCC-DFTB-D method. The initial geometries of dimers and pentamers were built considering the EPT-C2 and top-parallel alkane chain conformations, but subsequently, several "defects" (a perpendicular shift of the third monomer based on the EPT-C6 conformation and on the face-to-face conformation of EPT-C1) on these geometries were also taken into account. Several figures (Figures S1−S5, Supporting Information) showing different dimer and pentamer structures of PTZ + alkyl chains can be seen in the Supporting Information. Starting with geometry optimization from the initial geometry, regular dimers and pentamers were found, where the PTZ fragments have the VS form, while the alkane fragments

show the top-parallel conformation (see Figures S1(A), S1(C), and S3(A)−S3(D), Supporting Information). Considering the dimer structures of the decyl-PTZ and thio-nonyl-PTZ units built on the basis of EPT-C2 (Figures S1(A) and S1(C), Supporting Information) and EPT-C6 (Figures S1(B) and S1(B), Supporting Information) conformations, the following intermolecular interaction energy values were obtained: −17.4 kcal/mol for decyl-PTZ (I), −18.1 kcal/mol for decyl-PTZ (II), −17.5 kcal/mol for thio-nonyl-PTZ (I), and −16.7 kcal/mol in the case of thio-nonyl-PTZ (II). Here "I" stands for the PTZ-alkyl binary systems where the alkyl chains have the top-parallel configuration and "II" for the alkyl chains showing side-parallel geometry. The conformational energy differences are close to the magnitude of the thermal energy for both decyl-PTZ and thio-nonyl-PTZ dimers, with the Supporting Information that while in the first case the distorted dimer (decyl-PTZ (II)) shows a somewhat stronger interaction, in the second case the regular form has the energetically favored conformation. In the case of the decyl-PTZ structure a third dimer geometry (decyl-PTZ(III)) was also prepared taking into account the face-to-face conformation of PTZ fragments (see EPT-C1 on Figure 6) and the side-parallel form of the alkyl chains (Figure S2, Supporting Information). For this new structure we obtained −21.8 kcal/mol for the intermolecular interaction energy, 4.4 kcal/mol lower than the energy obtained for decyl-PTZ(I). This energy difference is quite important, and we consider it an undesired configuration which can worsen significantly the self-organization process.

In order to try to model potential distortions from the regular pentamer structure, further geometry optimizations were performed. Here, at the initial geometry, the third monomer was shifted in line with the second and forth monomers. Optimized structures are presented in Figures S1(B), S1(D), S4, and S5, Supporting Information. Considering the total energy values of the distorted pentamers and comparing them with similar energy values of the regular pentamer form, we found that all of distorted pentamers are energetically more favorable than the corresponding regular pentamers. In the case of the functional group shift, we obtained the following conformational energy differences: −1.0 kcal/mol for hexyl-PTZ (Figure S4(A), Supporting Information), −0.6 kcal/mol for thio-pentyl-PTZ (Figure S4(B), Supporting Information), −4.9 kcal/mol for decyl-PTZ (Figure S5(A), Supporting Information), and −4.5 kcal/mol for thio-nonyl-PTZ (Figure S5(C), Supporting Information). Extruding two monomers from the regular pentamer of decyl-PTZ we found a completely different conformation (see Figure S5(B), Supporting Information), where the alkyl chain of a dimer lies across on the residual trimmer alkyl chain. In this case the conformational energy difference is much larger (−15.1 kcal/mol) than the one found for the simple functional group shift.

4. Molecular Self-Association

The computational results allow us to predict the structure and behavior of PTZ derivatives when they self-organize in SAMs. As PTZ and its derivatives are insoluble in water in the SAMs fabrication processes one must use some organic solvents (acetone, alcohols, benzene, etc.) able to establish pairwise vdW and/or $\pi-\pi$ stacking solute−solvent molecular attraction. In spite of the fact that in our undertaking the solvent and the entropic effects are not taken into account (this aspect being the goal of our future research), the obtained results are strong arguments which allow us to predict with a reasonably high probability that the phenothiazine molecule and its derivatives are good candidates for self-assembling in supramolecular structures as monomolecular layers. Comparing the binding energy of the PTZ dimers with the binding energy of the benzene dimer, for example,[101] one can observe that the self-assembling cannot be hindered by the solvent. To be more specific, the binding energy of the EPT-C1 $\Delta E_{LMP2} = -13.9$ kcal/mol (the binding energy of the PTZ dimer is $\Delta E_{SCSN-LMP2} = -10.4$ kcal/mol) is about four times the binding energy of the benzene dimer corresponding to the most stable structure. Similar arguments allowed us to say that by adding the spacer and the linker the energetic balance becomes even more favorable to self-organization in larger aggregates. Accordingly, one can conclude that in dilute solution the quantum chemistry permits formation of bound molecular pairs, which tend to form larger ordered molecular aggregates and finally to self-associate in the well-known bidimensional SAM structure.

An interesting aspect of self-assembling is the degree of order that can be ensured in the supramolecular structure. The main parameter that is responsible for the high molecular order is the difference among the potential competitive structures. If the complexity of the molecular building block increases the number of potential defects appearing in the structure increases also. In this respect several defects have been investigated and their energies have been estimated. For defects that do not differ very much from the structure with the highest symmetry the calculated energy differences are not very large but can become sometimes favorable for the distorted structures. If the distortion becomes significant the difference between the energies are large enough and the nonregular structure seems to be more stable. Accordingly, one has to find out the optimal length of the alkyl chain which is long enough to facilitate the parallel aggregation (EPT-C2) of the PTZ aromatic rings but is reasonably short to not allow the appearance of the distorted oligomers. Adding together the attractive effects of the PTZ fragments, the constructive contributions of the top-parallel alkyl chain and of the thiol group as well as the destructive effect of the side-parallel alkyl chain we establish that the pentane chain has the optimal length. One should not forget also that in the case of longer alkyl chains the conformational isomers with more complex geometries (for example, nonlinear zigzag chain) could appear more frequently,[21] cases not taken into account in our investigation.

Finally, one must stress that all attempts must be improved by taking into account the constraint of the neighboring self-assembled *n*-mers, and consequently, the results calculated for the proposed structures are obtained in relatively restrictive hypotheses, accordingly a lot of computational effort must be added for more a realistic molecular environment.

A special comment must be added regarding the effect of the external constraint imposed by the geometry of the atomic lattice encountered by the organic molecules at the metallic surface. As we have shown, there are two distinct conformations associated with the relative positions of the alkyl chains. In order to minimize the intermolecular interaction energy and to adopt the side-parallel conformation the geometric relaxation of the molecular structure must be allowed so that the distance between the spacers is optimized. This goal is not very easy to achieve because it is difficult to satisfy the geometric restrictions given by the metallic surface on one side and the phenothiazine functional group on the other side simultaneously. The mismatch is usually minimized by tilting the chain at an optimal angle with respect to the normal at the atomically flat surface. Calculation of tilted structures, although computationally feasible, was left out from the present study, since their relevance

depends on the specific properties of the metallic crystalline lattice, which will be investigated in future work.

5. Conclusions

The intermolecular $\pi-\pi$ stacking interaction between some phenothiazine derivatives and between alkane chains with different lengths have been investigated using the Hartree−Fock and local second-order Møller−Plesset perturbation theory. Both methods have been combined with the coupled cluster (CC) and density functional (DFT) techniques. For all calculations, the correlation-consistent basis sets of cc-pVNZ (where N = D,T,Q) were used. Several hypothetical parallel and antiparallel stacking conformations were investigated. In all cases the stacking structures join together in a characteristic "V" form. It was found that the conformational stability of these molecular systems is exclusively given by the dispersion-type electron correlation effects. Considering the LMP2 geometry, the HF contribution in the intermolecular interaction energy gives positive values, acting as repulsion forces lacking the dimer structure. This effect is compensated by the larger contribution of dispersion forces, which finally keeps together the stacking structures. Accordingly, our prediction is that the process of self-assembling in supramolecular structures (such as monolayers, for example) having as the basic unit some phenothiazine derivatives might occur with a high probability if the length of the alkyl chain is properly chosen. All presumptions must also be validated by a comprehensive molecular dynamics simulation where the thermal and solvent effects are explicitly taken into account. Furthermore, several changes seem to be necessary in the structure of our molecular units for increasing their self-assembling ability. Therefore, based on the present results, we intend to design new molecular units. For instance, two carbon atoms in the PTZs rings could be replaced with nitrogen, which brings an enhancement of the $\pi-\pi$ stacking interaction. Additionally, if the central single alkyl chain could be replaced by two similar alkyl chains linked to benzene PTZs rings, the undesirable effect of the side-parallel configuration could be avoided.

Acknowledgment. This work was funded by the Romanian National Authority for Scientific Research through the CNCSIS Contract PCCE-ID_76. The computational infrastructure was provided through the INGRID Project No. POS-CCE-SMIS-192/2719. We gratefully acknowledge the technical assistance of the Data Center of NIRDIMT Cluj-Napoca.

Supporting Information Available: Additional figures with calculated results. This material is available free of charge via the Internet at http://pubs.acs.org.

References and Notes

(1) Dalgarno, S. J.; Tucker, S. A.; Bassil, D. B.; Atwood, J. L. *Science* **2005**, *309*, 203.
(2) Ghosh, S.; Wu, A.; Fettinger, J. C.; Zavalij, P. Y.; Isaacs, L. *J. Org. Chem.* **2008**, *73*, 5915.
(3) Kumara, M. T.; Nykypanchuk, D.; Sherman, W. B. *Nano Lett.* **2008**, *8*, 1971.
(4) Penadés, S.; de la Fuente, J. M.; Barrientos, Á. G.; Clavel, C.; Martínez-Ávila, O.; Alcántara, D. In *Nanomaterials for Application in Medicine and Biology*; Giersig, M., Khomutov, G. B., Eds.; Springer: Dordrecht, The Netherlands, 2008.
(5) Rajput, L.; Biradha, K. *CrystEngComm* **2009**, *11*, 1220.
(6) Verdan, S.; Melich, X.; Bernardinellib, G.; Williams, A. F. *CrystEngComm* **2009**, *11*, 1416.
(7) Jérome, D.; Shultz, H. *Adv. Phys.* **1982**, *31*, 299.
(8) Hunter, C. A.; Sanders, J. K. M. *J. Am. Chem. Soc.* **1990**, *112*, 5525.
(9) Kumpf, R. A.; Dougherty, D. A. *Science* **1993**, *261*, 1708.
(10) Müller-Dethlefs, K.; Hobza, P. *Chem. Rev.* **2002**, *100*, 143.
(11) Meyer, E. A.; Castellano, R. K.; Diederich, F. *Angew. Chem., Int. Ed.* **2003**, *42*, 1210.
(12) Hunter, C. A.; Singh, J.; Thornton, J. M. *J. Mol. Biol.* **1991**, *218*, 837.
(13) Saenger, W. *Principles of Nucleic Acid Structure*; Springer-Verlag: New York, 1984.
(14) Hobza, P. *Annu. Rep. Prog. Chem., Sect. C* **2004**, *100*, 3.
(15) Hunter, C. A. *Chem. Soc. Rev.* **1994**, *23*, 101.
(16) Kryger, G.; Silman, I.; Sussman, J. L. *J. Physiol.* **1998**, *92*, 191.
(17) Claessens, C. G.; Stoddart, J. F. *J. Phys. Org. Chem.* **1997**, *10*, 254.
(18) Glaser, R.; Dendi, L. R.; Knotts, N.; Barnes, C. L. *Cryst. Growth Des.* **2003**, *3*, 291.
(19) Lehn, J.-M. *Supramolecular Chemistry: Concepts and Perspectives*; VCH: New York, 1995.
(20) Járai-Szabó, F.; Aştilean, S.; Néda, Z. *Chem. Phys. Lett.* **2005**, *408*, 241.
(21) Love, J. C.; Estroff, L. A.; Kriebel, J. K.; Nuzzo, R. G.; Witheside, G. M. *Chem. Rev.* **2005**, *105*, 1103.
(22) Dou, R. F.; Ma, X. C.; Xi, L.; Yip, H. L.; Wong, K. Y.; Lau, W. M.; Jia, J. F.; Xue, Q. K.; Yang, W. S.; Ma, H.; Jen, A. K. *Langmuir* **2006**, *22* (7), 3049.
(23) Turdean, R.; Bogdan, E.; Terec, A.; Petran, A.; Vlase, L.; Turcu, I.; Grosu, I. *Centr. Eur. J. Chem.* **2009**, *7*, 111.
(24) Genwa, R. K.; Chouhan, A. *J. Chem. Sci.* **2004**, *116*, 339.
(25) Gresh, N.; Pullman, B. *Mol. Pharm.* **1986**, *29*, 355.
(26) Wainwright, M.; Crossley, K. B. *J. Chemother.* **2002**, *14*, 431.
(27) Müller, T. J. J. *Tetrahedron Lett.* **1999**, *40*, 6563.
(28) Spreitzer, H.; Daub, J. J. *Chem.—Eur. J.* **1996**, *2*, 1150.
(29) Kulkarni, A. P.; Zhu, Y.; Babel, A.; Wu, P.-T.; Jenekhe, S. A. *Chem. Mater.* **2008**, *20*, 4212.
(30) Komine, Y.; Ueda, Y.; Goto, T.; Fujihara, H. *Chem. Commun.* **2006**, *3*, 302.
(31) Morari, C.; Bogdan, D.; Turcu, I. *Centr. Eur. J. Phys.* **2009**, *7*, 332.
(32) Pitoňák, M.; Neogrády, P.; Řezáč, J.; Jurečka, P.; Urban, M.; Hobza, P. *J. Chem. Theory Comput.* **2008**, *4*, 1829.
(33) Šponer, J.; Riley, K. E.; Hobza, P. *Phys. Chem. Chem. Phys.* **2008**, *10*, 2595.
(34) Hill, G.; Forde, G.; Hill, N.; Lester Jr., W. A.; Sokalski, W. A.; Leszczynski, J. *Chem. Phys. Lett.* **2003**, *381*, 729.
(35) Rodríguez-Ropero, F.; Casanovas, J.; Alemán, C. *J. Comput. Chem.* **2008**, *29*, 69.
(36) Stone, A. J. *The Theory of Intermolecular Forces*; Oxford University Press: Oxford, 1997.
(37) Grimme, S. *Angew. Chem., Int. Ed.* **2008**, *47*, 3430.
(38) Rappé, A. K.; Bernstein, E. R. *J. Phys. Chem. A* **2000**, *104*, 6117.
(39) Allen, M.; Tozer, D. J. *J. Chem. Phys.* **2002**, *117*, 11113.
(40) Grimme, S. *J. Comput. Chem.* **2004**, *25*, 1463.
(41) Hobza, P.; Selzle, H. L.; Schlag, E. W. *J. Phys. Chem.* **1996**, *100*, 18790.
(42) Sinnokrot, M. O.; Valeev, E. F.; Sherrill, C. D. *J. Am. Chem. Soc.* **2002**, *124*, 10887.
(43) Tsuzuki, S.; Honda, K.; Uchimaru, T.; Mikami, M. *J. Chem. Phys.* **2004**, *120*, 647.
(44) Boys, S. B.; Bernardi, F. *Mol. Phys.* **1970**, *19*, 553.
(45) Mayer, I. *Int. J. Quantum Chem.* **1998**, *41*, 70.
(46) Bende, A.; Almásy, L. *Chem. Phys.* **2008**, *354*, 202.
(47) Ángyán, J. G.; Gerber, I. C. *Phys. Rev. A* **2005**, *72*, 012510.
(48) Gerber, I. C.; Ángyán, J. G. *J. Chem. Phys.* **2007**, *126*, 044103.
(49) Toulouse, J.; Colonna, F.; Savin, A. *J. Chem. Phys.* **2005**, *122*, 014110.
(50) Grimme, S. *J. Chem. Phys.* **2006**, *124*, 034108.
(51) Grimme, S. *J. Comput. Chem.* **2004**, *25*, 1463.
(52) Grimme, S. *J. Comput. Chem.* **2006**, *27*, 1787.
(53) von Lilienfeld, O.; Tavernelli, I.; Röthlisberger, U.; Sebastiani, D. *Phys. Rev. Lett.* **2004**, *93*, 153004.
(54) DiLabio, G. A. *Chem. Phys. Lett.* **2008**, 455–348.
(55) Jurečka, P.; Šponer, J.; Cerný, J.; Hobza, P. *P. Phys. Chem. Chem. Phys.* **2006**, *8*, 1985.
(56) Nilsson Lill, S. O. *J. Phys. Chem. A* **2009**, *113*, 10321.
(57) Mackie, I.; DiLabio, G. A. *J. Phys. Chem. A* **2008**, *112*, 10968.
(58) Mackie, I.; McClure, S. A.; DiLabio, G. A. *J. Phys. Chem. A* **2009**, *113*, 5476.
(59) Zhao, Y.; Truhlar, D. G. *Theor. Chem. Acc.* **2008**, *120*, 215.
(60) Pulay, P. *Chem. Phys. Lett.* **1983**, *100*, 151.
(61) Saebø, S.; Pulay, P. *Annu. Rev. Phys. Chem.* **1993**, *44*, 213.
(62) Hampel, C.; Werner, H.-J. *J. Chem. Phys.* **1996**, *104*, 6286.
(63) Hetzer, G.; Schütz, M.; Stoll, H.; Werner, H.-J. *J. Chem. Phys.* **2000**, *113*, 9443.
(64) Schütz, M. *J. Chem. Phys.* **2000**, *113*, 9986.
(65) Schütz, M.; Werner, H.-J. *J. Chem. Phys.* **2001**, *114*, 661.

(66) Vahtras, O.; Almlöf, J.; Feyereisen, M. W. *Chem. Phys. Lett.* **1993**, *213*, 514.
(67) Hill, J. G.; Platts, J. A.; Werner, H.-J. *Phys. Chem. Chem. Phys.* **2006**, *8*, 4072.
(68) Elstner, M.; Porezag, D.; Jungnickel, G.; Elsner, J.; Haugk, M.; Frauenheim, T.; Suhai, S.; Seifert, G. *Phys. Rev. B* **1998**, *58*, 7260.
(69) Elstner, M.; Jalkanen, K. J.; Knapp-Mohammady, M.; Frauenheim, T.; Suhai, S. *Chem. Phys.* **2000**, *256*, 15.
(70) Elstner, M.; Jalkanen, K. J.; Knapp-Mohammady, M.; Frauenheim, T.; Suhai, S. *Chem. Phys.* **2001**, *263*, 203.
(71) Elstner, M.; Hobza, P.; Frauenheim, T.; Suhai, S.; Kaxiras, E. *J. Chem. Phys.* **2001**, *114*, 5149.
(72) Liu, H. Y.; Elstner, M.; Kaxiras, E.; Frauenheim, T.; Hermans, J.; Yang, W. T. *Proteins: Struct., Funct., Genet.* **2001**, *44*, 484.
(73) Kubař, T.; Jurečka, P.; Černý, J.; Řezáč, J. ; Otyepka, M.; Valdés, H.; Hobza, P. *J. Phys. Chem. A* **2007**, *111*, 5642.
(74) MOLPRO, version2008. 1, a package of ab initio programs, Werner, H.-J.; Knowles, P. J.; Lindh, R.; Manby, F. R.; Schütz, M.; Celani, P.; Korona, T.; Mitrushenkov, A.; Rauhut, G.; Adler, T. B.; Amos, R. D.; Bernhardsson, A.; Berning, A.; Cooper, D. L.; Deegan, M. J. O.; Dobbyn, A. J.; Eckert, F.; Goll, E.; Hampel, C.; Hetzer, G.; Hrenar, T.; Knizia, G.; Köppl, C.; Liu, Y.; Lloyd, A. W.; Mata, R. A.; May, A. J.; McNicholas, S. J.; Meyer, W.; Mura, M. E.; Nicklass, A.; Palmieri, P.; Pflüger, K.; Pitzer, R.; Reiher, M.; Schumann, U.; Stoll, H.; Stone, A. J.; Tarroni, R.; Thorsteinsson, T.; Wang, M.; Wolf, A. Available from http://www.molpro.net.
(75) Dunning, T. H., Jr. *J. Chem. Phys.* **1989**, *90*, 1007.
(76) Kendall, R. A.; Dunning, T. H., Jr.; Harrison, R. J. *J. Chem. Phys.* **1992**, *96*, 6796.
(77) Mata, R. A.; Werner, H.-J. *Mol. Phys.* **2007**, *105* (19−22), 2761.
(78) Pipek, J.; Mezey, P. G. *J. Chem. Phys.* **1989**, *90*, 4916.
(79) Schütz, M.; Rauhut, G.; Werner, H.-J. *J. Phys. Chem.* **1998**, *102*, 5197.
(80) Bylaska, E. J.; de Jong, W. A.; Govind, N.; Kowalski, K.; Straatsma, T. P.; Valiev, M.; Wang, D.; Apra, E.; Windus, T. L.; Hammond, J.; Nichols, P.; Hirata, S.; Hackler, M. T.; Zhao, Y.; Fan, P.-D.; Harrison, R. J.; Dupuis, M.; Smith, D. M. A.; Nieplocha, J.; Tipparaju, V.; Krishnan, M.; Vazquez-Mayagoitia, A.; Wu, Q.; Van Voorhis, T.; Auer, A. A.; Nooijen, M.; Crosby, L. D.; Brown, E.; Cisneros, G.; Fann, G. I.; Fruchtl, H.; Garza, J.; Hirao, K.; Kendall, R.; Nichols, J. A.; Tsemekhman, K.; Wolinski, K.; Anchell, J.; Bernholdt, D.; Borowski, P.; Clark, T.; Clerc, D.; Dachsel, H.; Deegan, M.; Dyall, K.; Elwood, D.; Glendening, E.; Gutowski, M.; Hess, A.; Jaffe, J.; Johnson, B.; Ju, J.; Kobayashi, R.; Kutteh, R.; Lin, Z.; Littlefield, R.; Long, X.; Meng, B.; Nakajima, T.; Niu, S.; Pollack, L.; Rosing, M.; Sandrone, G.; Stave, M.; Taylor, H.; Thomas, G.; van Lenthe, J.; Wong, A.; Zhang, Z. *NWChem, A Computational Chemistry Package for Parallel Computers*, Version 5.1.1; Pacific Northwest National Laboratory: Richland, WA, 2009.
(81) DFTB+ 1.0.1 is a DFTB implementation, which is free for noncommercial use. For details, see: http://www.dftb-plus.info.
(82) Aradi, B.; Hourahine, B.; Frauenheim, T. *J. Phys. Chem. A* **2007**, *111* (26), 5678.
(83) Allouche, A.-R. *J. Comput. Chem.* **2010**, (in press), doi: 10.1002/jcc.21600. Available from http://gabedit.sourceforge.net/.
(84) Grimme, S. *J. Chem. Phys.* **2003**, *118*, 9095.
(85) Hill, J. G.; Platts, J. A. *J. Chem. Theory Comput.* **2007**, *3*, 80.
(86) Johnson, E. R.; Becke, A. D.; Sherrill, C. D.; DiLabio, G. A. *J. Chem. Phys.* **2009**, *131*, 034111.
(87) Mackie, I. D.; DiLabio, G. A. *Phys. Chem. Chem. Phys.* **2010**, *12*, 6092.
(88) Hohenstein, E. G.; Chill, S. T.; Sherrill, C. D. *J. Chem. Theory Comput.* **2008**, *4*, 1996.
(89) Sherrill, C. D.; Sumpter, B. G.; Sinnokrot, M. O.; Marshall, M. S.; Hohenstein, E. G.; Walker, R. C.; Gould, I. R. *J. Comput. Chem.* **2009**, *30*, 2187.
(90) Řezáč, J.; Fanfrlik, J.; Salahub, D.; Hobza, P. *J. Chem. Theory Comput.* **2009**, *5*, 1749.
(91) Korth, M.; Pitoňák, M.; Řezáč, J.; Hobza, P. *J. Chem. Theory Comput.* **2010**, *6*, 344.
(92) Stewart, J. J. P. *J. Mol. Modeling* **2007**, *13*, 1173.
(93) Stewart, J. J. P. *MOPAC2009*; Stewart Computational Chemistry: Colorado Springs, CO, 2008; http://OpenMOPAC.net.
(94) Allinger, N. L.; Yuh, Y. H.; Lii, J.-H. *J. Am. Chem. Soc.* **1989**, *111*, 8551.
(95) Tinker 5.1 molecular modeling software; http://dasher.wustl.edu/tinker.
(96) Ren, P.; Ponder, J. W. *J. Comput. Chem.* **2002**, *23*, 1497.
(97) Ren, P.; Ponder, J. W. *J. Phys. Chem. B* **2003**, *107*, 5933.
(98) Bende, A.; Turcu, I. *J. Phys: Conf. Ser.* **2009**, *182*, 012001.
(99) Tsuzuki, S.; Honda, K.; Uchimaru, T.; Mikami, M. *J. Phys. Chem. A* **2004**, *108*, 10311.
(100) Tsuzuki, S.; Honda, K.; Uchimaru, T.; Mikami, M. *J. Chem. Phys.* **2006**, *124*, 114304.
(101) von Lilienfeld, O. A.; Andrienko, D. *J. Chem. Phys.* **2006**, *124* (5), 054307.

JP105012G

Supporting Information:

Molecular modeling of phenothiazine derivatives self-assembling properties

Attila Bende,*,† Ion Grosu,‡ and Ioan Turcu†

Molecular and Biomolecular Physics Department, National Institute for Research and Development of Isotopic and Molecular Technologies, Donath Street, No. 65-103, Ro-400293 Cluj-Napoca, Romania., and Chair of Organic Chemistry, Faculty of Chemistry and Chemical Engineering, "Babeş-Bolyai" University, Arany Janos Street, No. 11, Ro-400028, Cluj-Napoca, Romania.

E-mail: bende@itim-cj.ro

*To whom correspondence should be addressed

†Molecular and Biomolecular Physics Department, National Institute for Research and Development of Isotopic and Molecular Technologies, Donath Street, No. 65-103, Ro-400293 Cluj-Napoca, Romania.

‡Chair of Organic Chemistry, Faculty of Chemistry and Chemical Engineering, "Babeş-Bolyai" University, Arany Janos Street, No. 11, Ro-400028, Cluj-Napoca, Romania.

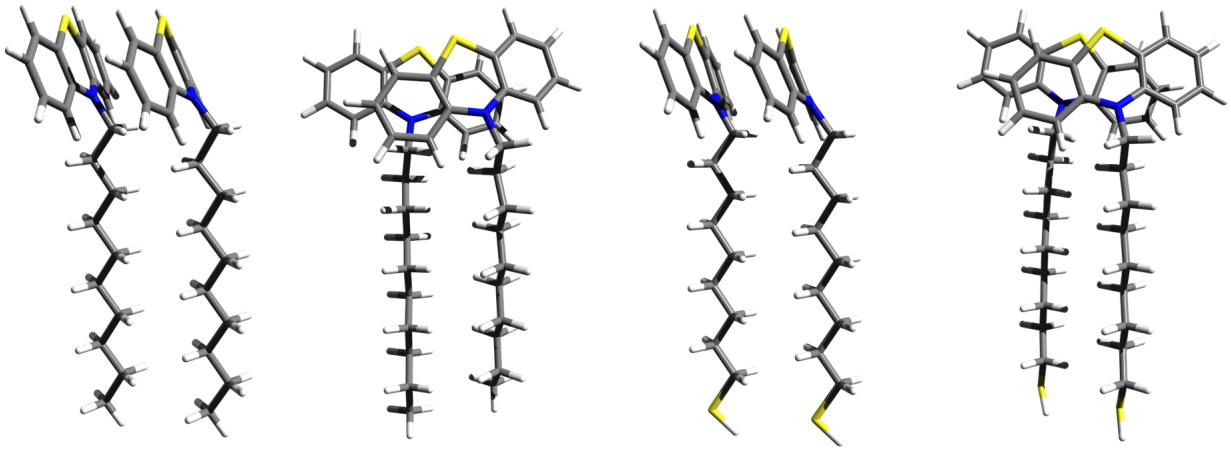

A: decyl-PTZ (I) **B:** decyl-PTZ (II) **C:** thio-nonyl-PTZ (I) **D:** thio-nonyl-PTZ (II)

Figure S1. The parallel and shifted (defected) dimers of decyl-PTZ and thio-nonyl-PTZ.

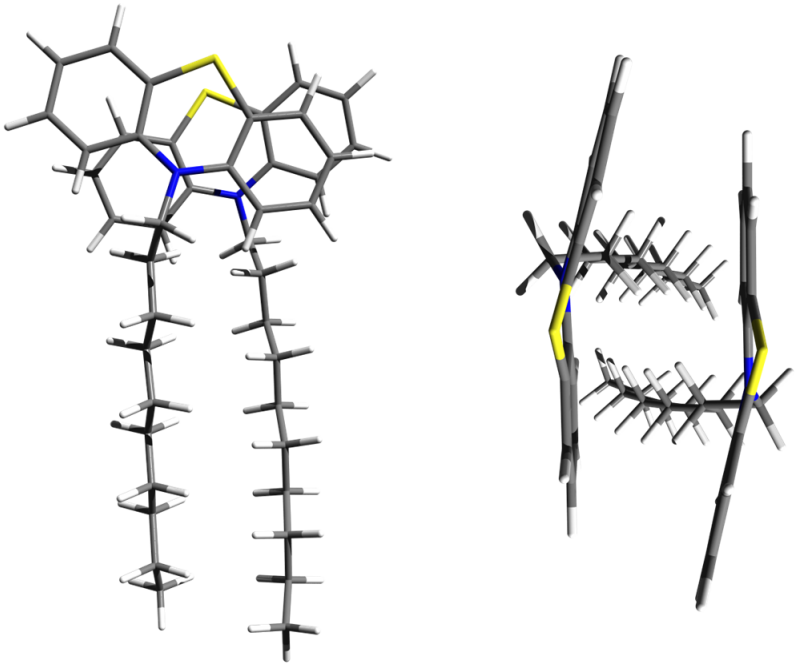

decyl-PTZ (III)

Figure S2. The face-to-face defected dimer of decyl-PTZ.

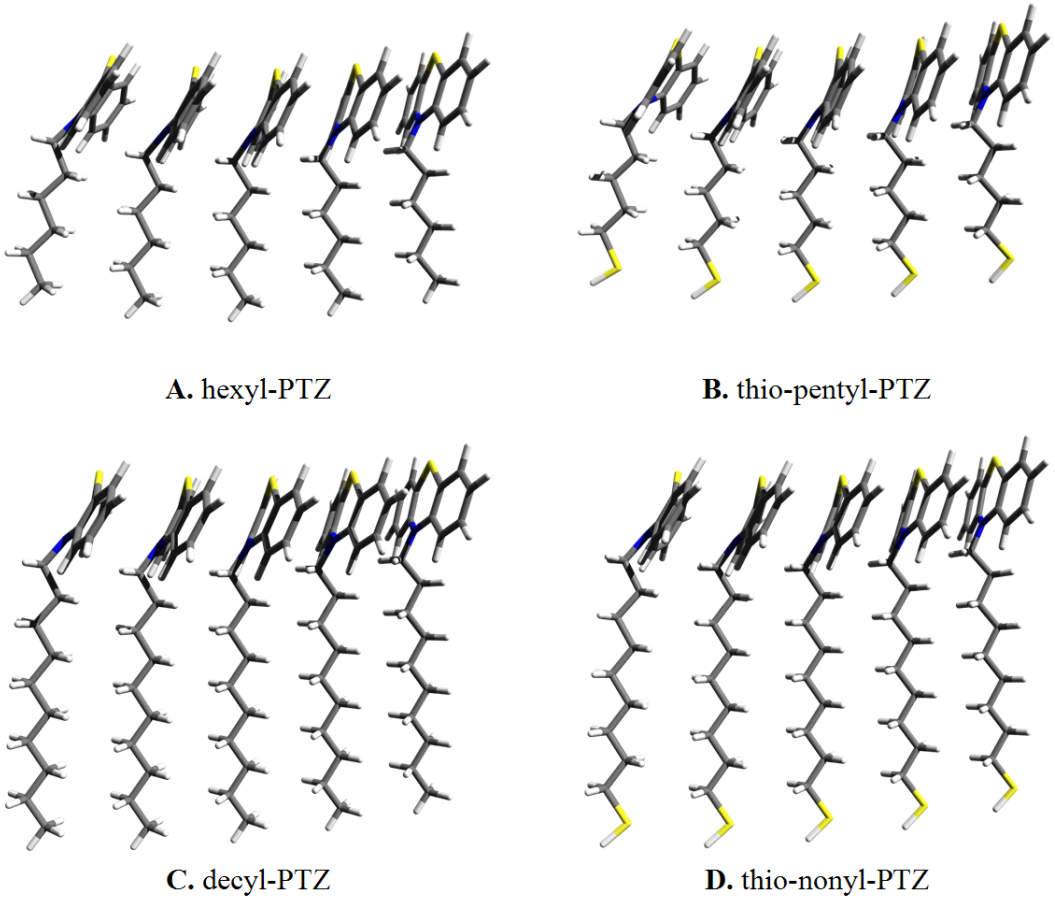

Figure S3. The pentamers of decyl-PTZ and thio-nonyl-PTZ.

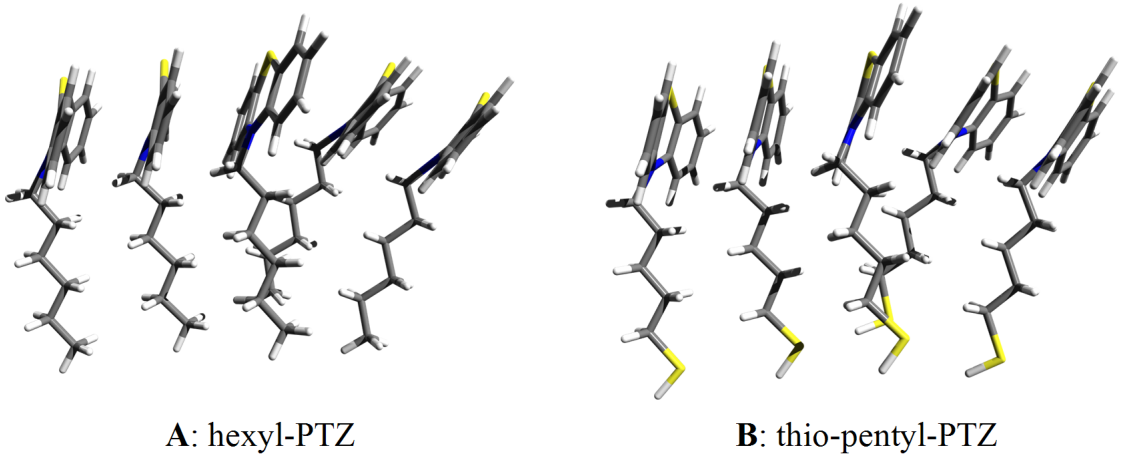

Figure S4. Some "defected" pentamers of hexyl-PTZ and thio-pentyl-PTZ.

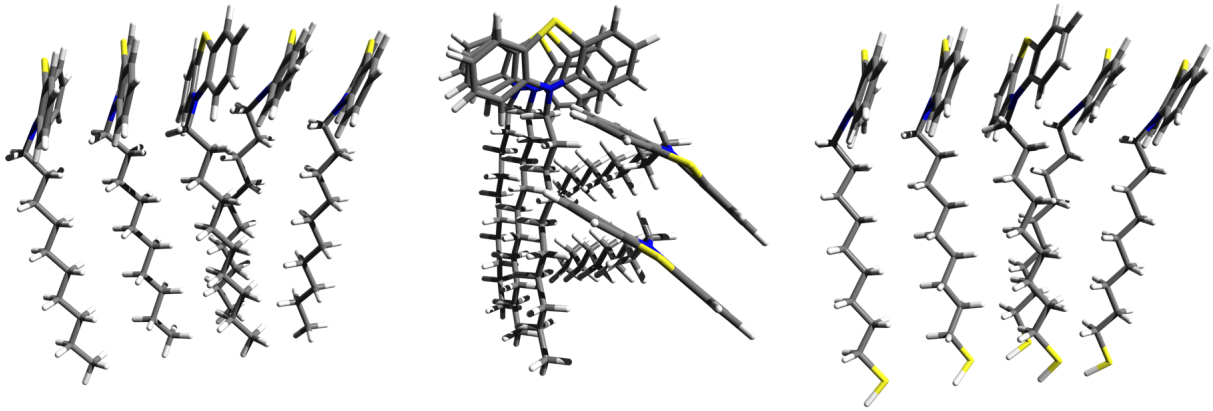

A: decyl-PTZ (a) **B**: decyl-PTZ (b) **C**: thio-nonyl-PTZ

Figure S5. Some "defected" pentamers of decyl-PTZ and thio-nonyl-PTZ.